Hindawi
Advances in Materials Science and Engineering
Volume 2019, Article ID 3268276, 10 pages
https://doi.org/10.1155/2019/3268276

Research Article

Effect of Cyclic Expansion-Extrusion Process on Microstructure, Deformation and Dynamic Recrystallization Mechanisms, and Texture Evolution of AZ80 Magnesium Alloy

Yong Xue, Shuaishuai Chen, Haijun Liu, Zhimin Zhang, Luying Ren, and Bing Bai

School of Material Science and Engineering, North University of China, No. 3 Xueyuan Rd., Taiyuan 030051, China

Correspondence should be addressed to Yong Xue; yongxue395@163.com

Received 25 August 2018; Accepted 3 January 2019; Published 5 February 2019

Academic Editor: Patrice Berthod

The microstructure, deformation mechanisms, dynamic recrystallization (DRX) behavior, and texture evolution of AZ80 magnesium alloy were investigated by three-pass cyclic expansion-extrusion (CEE) tests. Optical microscopy (OM), electron back-scattered diffraction (EBSD), and X-ray diffraction (XRD) were employed to study microstructure, grain orientation, DRX mechanism, and texture evolution. The results show that the grain sizes decrease continuously with the increase of CEE pass. The grain refinement effect of the first pass is the most remarkable, and there appear a large number of twins. After three-pass CEE, a well-distributed structure with fine equiaxed grains is obtained. With the increase of CEE pass, the deformation mechanism changes from twinning to slipping and the DRX mechanism changes mainly from twinning-induced dynamic recrystallization (TDRX) to rotation dynamic recrystallization (RDRX) and then to continuous dynamic recrystallization (CDRX). The grain misorientation between the new grains and matrix grains deceases gradually, and a relatively small angle misorientation is obtained after three-pass CEE. Grain misorientations of the first two passes are attributed to TDRX and RDRX behaviors, respectively. The grain refinement changes the deformation and DRX mechanisms of CEE process, which leads the (0002) basal texture intensity first decrease and then increase suddenly. Eventually, the extremely strong basal texture is formed after three-pass CEE.

1. Introduction

Due to their low weight, high specific strength, and fatigue strength, magnesium alloys have attracted significant interests in a variety of technology-related applications, especially in automotive and aerospace products [1, 2]. It is well known that most magnesium alloys are hard to deform at room temperature owing to their hexagonal close-packed (HCP) structure and limited slip modes [3]. The severe plastic deformation at high temperature can refine the grains size, which will improve the deformation ability at room temperature of the alloy. So, a considerable amount of researches have been focused on the hot deformation behavior of Mg alloy to obtain desirable microstructure and mechanical properties [4, 5].

In the past few years, various techniques have been developed to improve the mechanical performance of magnesium alloy, such as high-pressure torsion (HPT) [6], equal channel angular press (ECAP) [7], cyclic extrusion compression (CEC) [8], and cyclic expansion-extrusion (CEE) [9, 10]. CEE is a relatively new severe plastic deformation technique. During CEE, severe plastic deformation is applied to the material, and significant grain refinement was achieved [11], which will enhance the mechanical performance of the studied alloy. Except for grain refinement, CEE can change the deformation mechanism and texture intensity of material. Slipping and twinning are two major deformation mechanisms of Mg alloy [12] and can significantly affect the texture evolution [13]. Hu et al. [14] and Wang et al. [15] pointed out that typical basal texture can be found in extruded magnesium alloy. Twinning can adjust the grain orientations of the Mg alloy and activate more nonbasal slip systems [16–18], which is benefit to the deformation of the alloy. Xin et al. [19] revealed that

twinning can help the homogeneous plastic deformation of Mg alloy. During the thermal-mechanical processing of Mg alloy, dynamic recrystallization is an important way to refine the grain size [5]. The common dynamic recrystallization mechanism of the Mg alloy includes twinning-induced dynamic recrystallization, continuous dynamic recrystallization, and rotation dynamic recrystallization [20–22], which makes the microstructural evolution more complex. Sheikh and Ebrahimi [23] studied the texture evolution during CEE technique using crystal plasticity finite element modeling. However, there is little research work focusing on the texture evolution of Mg alloy during CEE technique. So deep studies about twinning, grain orientation, and DRX mechanism contribute to the understanding of the microstructural and texture evolution of Mg alloy during CEE.

In this study, the multipass CEE deformation behaviors of annealed AZ80 magnesium alloy were comprehensively studied at the CEE temperature of 623 K. With the help of OM, EBSD, and XRD technologies, microstructure observations were carried out to analyze the twinning, crystallographic orientation, and DRX behavior during CEE process and the relationship between CEE and texture evolution is investigated.

2. Materials and Experiments

A commercial cast AZ80 Mg alloy is used in this study. The composition of the as-received alloy is given in Table 1. Prior to the CEE process, the homogenized annealing treatment was carried out at 673 K for 15 h to eliminate arborescent structure and composition segregation. The sample with a cross section of 100 mm × 50 mm, and 170 mm in length was machined from the annealed material. The THP61.630 hydraulic machine was employed to perform the three-pass CEE tests. The die used in the CEE tests was made up of punch, block, upper female die, lower female die, upper plate, and lower plate, as shown in Figure 1.

Before the CEE test, the die was heated to 673 K and the samples were heated to 623 K. The graphite was used to reduce friction between the samples and die. The schematic diagram of the CEE test is shown in Figure 2. The CEE process consists of two steps, as depicted in Figure 2(a), i.e., expansion and extrusion. During the CEE process, the expansion and extrusion steps take place on different planes, which are normal to each other (Figure 2(a)). By closing the output channel with the block, the die is filled up with sample A firstly (Figure 2(b)), and the cross section of sample A expands from 50 mm × 100 mm to 100 mm × 100 mm. Then, the block is removed and sample B is put into the inlet channel. The cross section of sample A is extruded from 100 mm × 100 mm to 100 mm × 50 mm, and the expanded sample A retrieves its initial geometry in the extrusion stage of the CEE process (Figure 2(c)). This process is repeated several times to reach the desired number of passes (Figure 2(d)). In this work, the expansion and extrusion steps during CEE process were performed on different planes, which are normal to each other, as Routes II mentioned in the work of Pardis et al. [10]. The whole CEE process was performed three times, and the deformed samples were used to analyze the effect of CEE on the microstructural evolution of the studied AZ80 alloy.

Table 1: Chemical composition of the cast AZ80 Mg alloy (wt.%).

Al	Zn	Mn	Fe	Cu	Si	Ni	Mg
7.80–9.20	0.20–0.80	0.12–0.5	0.005	0.05	0.1	0.005	Bal.

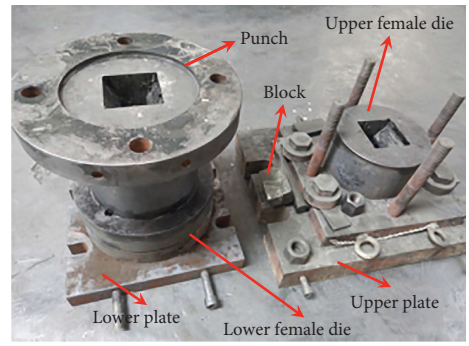

Figure 1: Drawing of the CEE die.

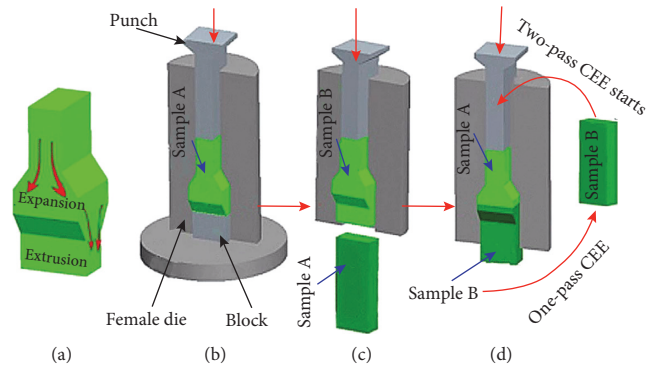

Figure 2: Schematic diagram of the CEE test.

The expansion and extrusion steps during CEE process were performed on different planes, which are normal to each other.

The samples used for the microstructural observation were taken from the longitudinal section of the CEE deformed sample, as shown in Figure 3. The optical microstructure of the samples was analyzed by using the ZEISS image metallographic microscope. The EBSD study was conducted on SU5000 scanning electron microscopy (SEM) equipped with an EBSD testing system. The (0002) and (10-10) texture was measured by using the D-5000 X-ray test system, and Matlab 2014 software was used to analyze the test data.

3. Results and Discussion

3.1. Effect of CEE on Microstructures. Figure 4 shows the optical microscope photographs of the annealed and 1–3 pass CEE samples. It is clearly found from Figure 4 that the grains are continuously refined and recrystallized during the CEE process. For the annealed Mg alloy, as shown in

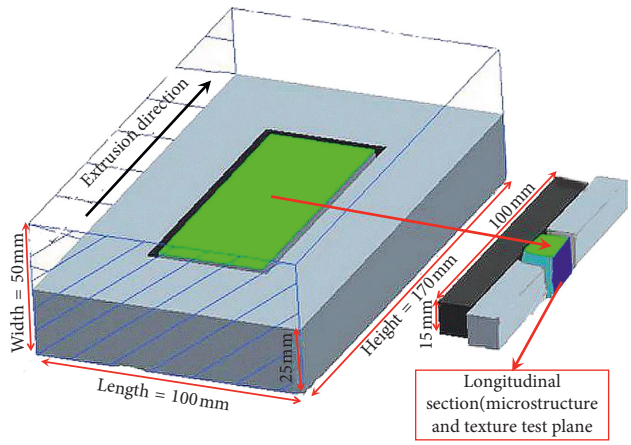

Figure 3: Schematic of sampling position in the deformed sample.

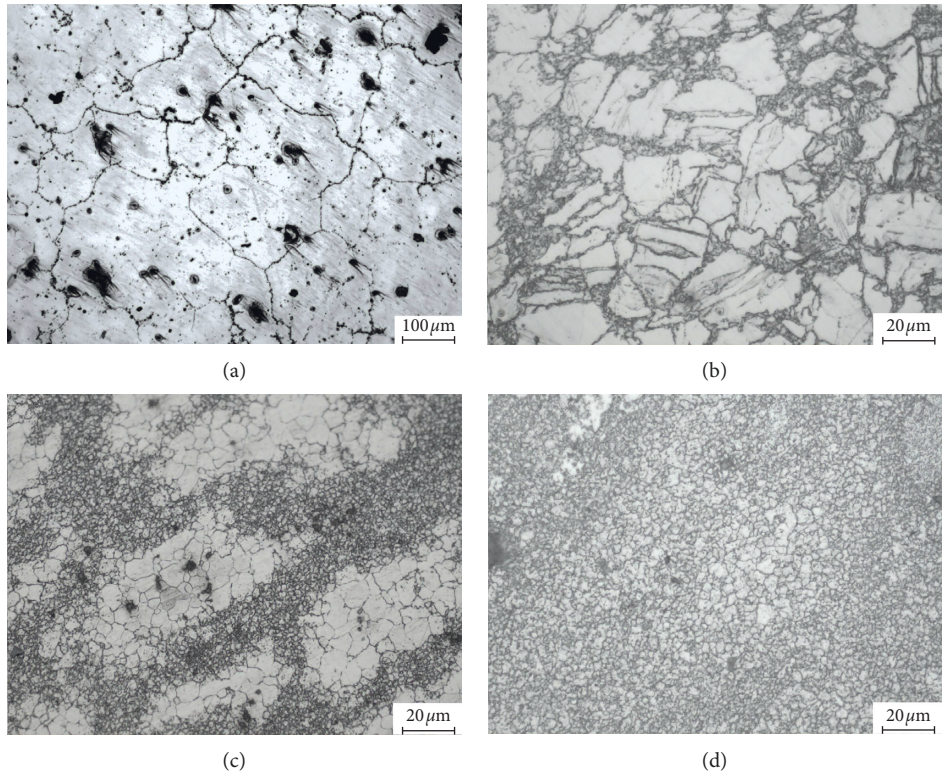

Figure 4: Optical microscope photograph of the samples: (a) the annealed; (b) one-pass CEE; (c) two-pass CEE; (d) three-pass CEE.

Figure 4(a), the structure mainly consists of coarse grains with a dimension of 150–230 μm approximately. After one-pass CEE, as shown in Figure 4(b), there appear a large number of lens-shaped twins crossing over almost all coarse grains, which contributes to remarkably refine the previous coarse grains. The lens-like twins are usually considered to be {10–12} tension twins, which mainly occurs in the early stage of deformation and contributes to the further strain [24]. It is noteworthy that, massive fine grains are produced within lens-like twins and lamellar-flake twins. The above structure features indicate that it is twinning that mainly induces the dynamic nucleation and growth, resulting in the grain refinement. Twinning deformation is a very important intragranular plastic deformation mechanism in the HCP lattice structure magnesium alloy. It helps us to activate the nonbasal slip and release stress concentration [25]. Moreover, Figure 4(b) shows that the necklace structure took place after one pass of CEE. It is attributed to the DRX mechanism changes from the twinning-induced dynamic recrystallization (TDRX) to the early stage of continuous dynamic recrystallization (CDRX) [9, 20].

After two-pass CEE, the grains are further refined, as shown in Figure 4(c), the coarse grain size is less than 10 μm, and the fine grains are especially tiny. The coarse grains are surrounded by massive fine grains, and there appears local severe deformation zone with fine grains. The previous twins

almost completely disappear. The above microscopic morphology is highly consistent with the microstructure characteristic of the RDRX mechanism proposed by Ion et al. [26]. The RDRX mechanism holds that the new fine grains along or around the boundaries of initial coarse grains are first formed from the rotation of the initial subgrains. The orientation of new grains is greatly different from that of initial grains, forming a large deformation belt or ductile shear zone. It can be inferred that the RDRX behavior is dominant during two-pass CEE. This inference will be further demonstrated with the aid of misorientation between new grains and matrix grains, as showed in Section 3.2.

Figure 4(d) shows that a well-distributed structure with grain size of about 5 μm is obtained after multiple passes CEE deformation. The relatively coarse grains of two-pass CEE completely disappeared. Significant grain refinement is achieved with the increase of CEE pass. The essence of the CEE process is repeatedly expansion-extrusion deformation, and hence, the grain is continuously crushed and smashed, recrystallized, and refined, achieving final structure refinement.

3.2. Effect of CEE on Deformation and DRX Mechanisms. Figure 5 shows the orientation map of the annealed sample. Here, the different color levels stand for the different crystallographic orientation. The low-angle grain boundaries (LAGBs), boundaries of misorientation between 2° and 10°, are marked with thin white lines. The high-angle grain boundaries (HAGBs), boundaries above 10°, are marked with thick black lines. As can be seen from Figure 5, the particularly coarse equiaxed grains with HAGBs can be clearly found, and the orientation of the grains is nearly random.

Figure 6 shows the orientation map of the deformed sample after one-pass CEE. The boundaries of different twinning modes are distinguished by different colored lines. The {10–12} extension twin boundaries, {10–13} contraction twin boundaries, and {10-11} contraction twin boundaries are marked with red, blue, and green lines, respectively. From Figure 6, a lot of {10–12} and {10–13} twin boundaries and a few {10-11} twin boundaries are clearly observed. Besides, there are a lot of LAGBs and new fine grains form near these twin boundaries. From the features of the orientation map (Figure 6) and metallographic structure (Figure 4(b)), it can be considered that TDRX behavior is the main mechanism of grain refinement. Because of the low critical resolved shear stress (CRSS), {10–12} extension twinning most easily occurs at the initial stages of deformation of Mg alloy, contributing to release of stress and further slip deformation [24]. In general, when magnesium alloy is under a tension stress along *c*-axis direction of HCP lattice or a compression stress perpendicular to the *c*-axis direction, the {10–12} extension twinning usually occurs [26]. The {10–13} contraction twinning plays an important role when the applied contraction stress is along the *c*-axis direction [27]. The {10–12}, {10–13} and {10-11} twinning deformation can cause the reorientation of the *c*-axis of HCP lattice, which leads to the formation of misorientation

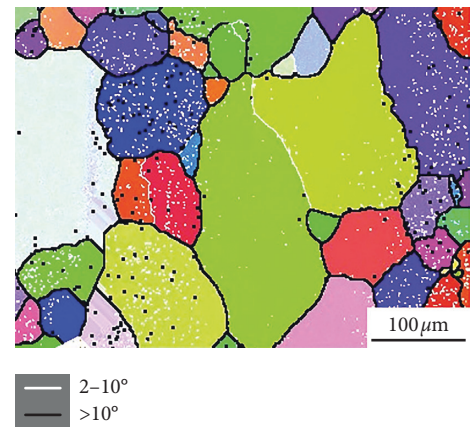

Figure 5: Orientation map of the annealed sample.

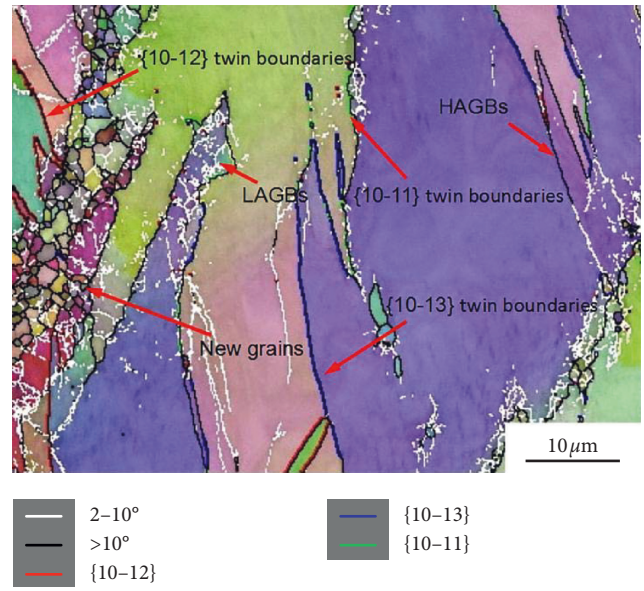

Figure 6: Orientation map of the sample after one-pass CEE.

between twins and matrix (86°, 64°, and 56°) [28]. During the CEE process, the alloy experiences the orthogonal expansion and extrusion deformation, which will generate complex stress field in the alloy. So, the {10–12} extension twin boundaries and {10–13} and {10-11} contraction twin boundaries are found in Figure 6.

After two-pass CEE, the grains are further refined and more fine equiaxed grains can be found, as shown in Figure 7. Similar to Figure 4(c), a large number of fine recrystallized grains are formed around the coarse grains. In order to further verify the RDRX behavior during two-pass CEE, this section employs the analysis methods of misorientation between the initial coarse grains and new fine grains. From the analyses of Figures 7 and 8(b), the orientation of new fine grains is obviously different from that of the initial coarse grains, which indicates new grains is produced by the RDRX behavior. Besides, in general, there are two kinds of nucleation modes at the grain boundary, subgrain rotation mechanism and grain boundary bulged-out mechanism. From the arrangement of fine grains at the

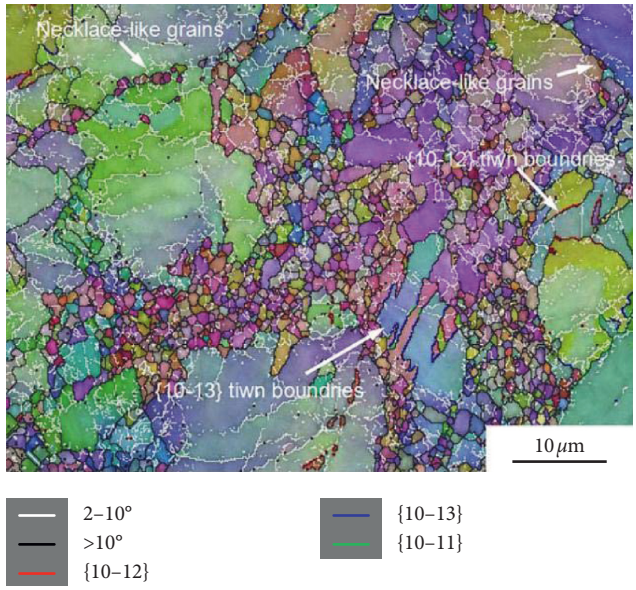

Figure 7: Orientation map of the samples after two-pass CEE.

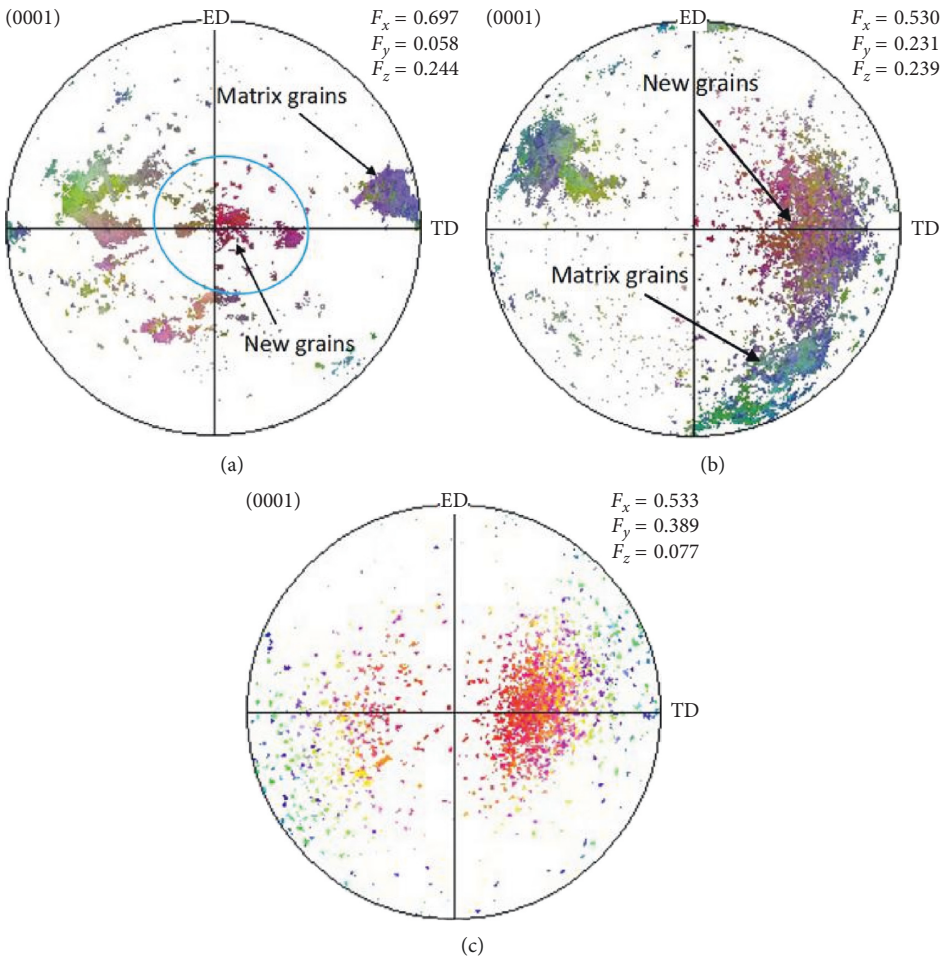

Figure 8: {0001} pole figure of the samples after CEE process: (a) one-pass; (b) two-pass; (c) three-pass.

grain boundaries, the nucleation mode can be judged as subgrain rotation mechanism because it is easily observed that the necklace-like fine grains are widely distributed at boundaries of coarse grains as shown in Figure 7. These fine grains are distributed on both sides of the grain boundaries, and there are hardly serrate-like grain boundaries or bulged-

out boundaries from one side to the other. Galiyev et al. [29] pointed out that the necklace-like grains are grown up from the subgrain nucleation. Substructure was initially formed at the initial coarse grain boundaries and then rotated and merged into fine recrystallized grains with high-angle grain boundaries. Therefore, it is easily concluded that the RDRX is the main recrystallization mechanism. During two-pass CEE, the sample passed through the orthogonal expansion-extrusion channel, undergoing severe shearing deformation.

Moreover, a few {10–12} twin boundaries (red line), {10–13} twin boundaries (blue line), and {10–11} twin boundaries (green line) can still be found within some coarse grains, as shown in Figure 7, and the twin boundary almost completely disappear in the fine grains. On the whole, compared with one-pass CEE, the number of twin boundaries greatly decreases after the two-pass CEE. This is because the activation of twinning deformation strongly depends to the grain size [30]. Kaibyshev et al. [31] considered that the grain refinement of initial structure of Mg alloy can inhibit twinning. With the decrease of grain size, the interfacial energy of twin grains increases and the nucleation number of twin grains decreases. In the coarse grain, the distance of dislocation slip is relatively long and the stress easily concentrates at HAGBs, which benefits the nucleation of twins [24]. In the fine grain, however, the distance of the dislocation slip is short, and the grain refinement can activate nonbasal slip and grain boundary slip, which can effectively release the stress concentration. The concentrated stress is hard to exceed the critical shear stress of twin nucleation, and the twinning is restrained [30]. As a result, twinning plays a minor role during the two-pass CEE.

Figure 9 shows that a uniform fine grain structure is obtained after three-pass CEE. As seen in Figure 8(c), the crystal orientation of structure tends to be consistent. Besides, from the analysis of Figure 10(b), the misorientation angle from 2° to 45° accounts for about 70%. The small angle misorientation indicates that the new recrystallized grains are formed by migration of the subgrain boundaries, which is responsible for the CDRX behavior [32]. Besides, in Figure 9, a few residual LAGBs can still be observed and almost all of LAGBs cross over the grains, which can further demonstrate the occurrence of CDRX behavior. It is well known that slipping and twinning are the two most common deformation modes of magnesium alloys; they coordinate and compete with each other to promote continuous deformation. From Figure 9, the twins have disappeared completely, which attributes to that the significant grain refinement intensely inhibits twinning deformation. It means that slip deformation has completely become the deformation mechanism during the three-pass CEE process.

3.3. Grain Orientation during CEE Process. Figure 8 shows the {0001} pole figure of the samples after the 1–3 pass CEE by EBSD in the ED-TD plane with the normal direction (ND). It can be found from Figure 8(a) that the *c*-axis of matrix grains is nearly parallel to the ED-TD plane, while the *c*-axis of new recrystallized grains is nearly parallel to the ND direction. The misorientation between the new grains and

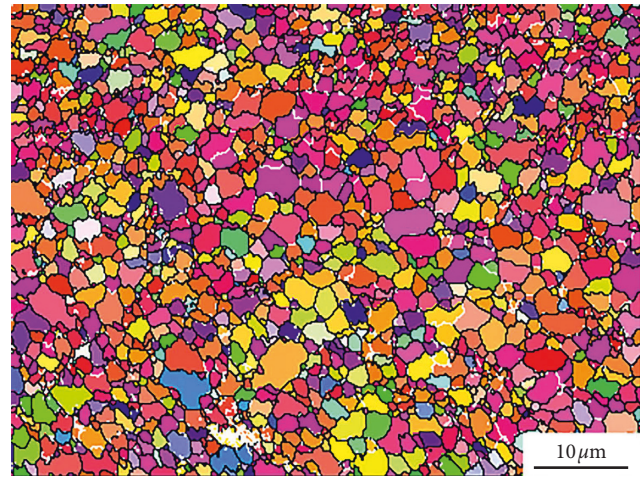

Figure 9: Orientation map of the sample after three-pass CEE.

the matrix grains is caused by TDRX behavior during the one-pass CEE process. As discussed in Section 3.2, the {10–12} extension twinning and {10–13} and {10–11} contraction twinning can rotate c-axis and cause the misorientation between the twin grains and the matrix (86°, 64°, and 56°). It is supported by Figures 8(a) and 10(a). In Figure 8(a), the misorientation of the new grains and the matrix grains is close to the 90-degree angle; Figure 10(a) shows the misorientation distribution map, and the misorientation angles are mainly composed of LAGBs and HAGBs (0–10°, approximately 60° and 85°), which strongly suggests that the existence of 86°{10–12} and 64°{10–13} twins. During the plastic deformation, slip dislocations are easily tangled at the twin boundaries [32, 33], which will lead to the formation of subgrains or LAGBs, as shown in Figures 6 and 10(a). It is because of the above multiple TDRX behaviors the c-axis of new recrystallized grains enormously deviates from that of matrix grains, and the HAGBs (more than 45°) account for about 60%, as shown in Figure 10(a).

Figure 8(b) shows the two-pass pole figure. It can be found from Figure 8(b) that there still exists distinctly misorientation between new recrystallized grains and the matrix grains. The RDRX behavior promotes the formation of the mixed structure with coarse grains and fine grains, impels the grain refinement, rotates the c-axis, and readjusts the orientation of new recrystallized grains [20]. The fine grain structure formed by RDRX can activate the nonbasal slip and grain boundary slip [30], and coarse grain structure still retains twinning deformation. All of the above factors make the deformation mechanism more complicated. The twinning and RDRX can cause the rotation of HCP lattice and change the grain orientation, leading to the misorientation between new recrystallized grains and the matrix grains.

The {0001} pole figure of the sample after three-pass CEE process is shown in Figure 8(c). It can be found from Figure 8(c) that the grain orientation of structure tends to be consistent. After the first two-pass CEE deformation, the great grain refinement effectively restrains the twinning deformation (Figure 7). At this time, as discussed above, slip deformation has completely become the deformation

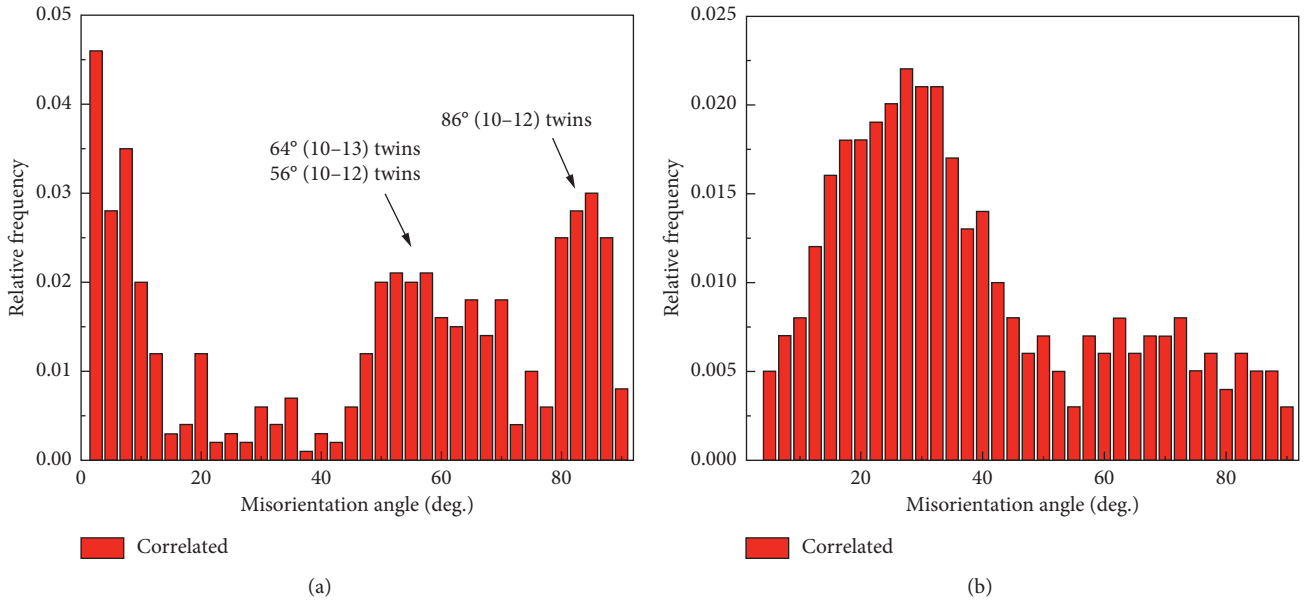

Figure 10: Misorientation distribution map of the studied alloy after CEE process: (a) one-pass; (b) three-pass.

mechanism. Vast literatures have showed that a particular plastic deformation mode can cause a specific texture. For instance, the samples extruded through ECAP process obtained the strong {0001} basal texture [34], or it was found that the strong {0001} basal texture is widely distributed on the rolling plane for as-rolled magnesium alloy [35]. Similarly to extrusion process, the CEE process may obtain the correlate deformation texture and cause the preferred orientation. But, slipping cannot deflect the *c*-axis of HCP lattice and not effectively reduce the preferred orientation [16]. Eventually, the relatively small angle misorientation is formed after three-pass CEE, as shown in Figure 10(b); the misorientation angle from 2° to 45° accounts for about 70%.

3.4. Effect of CEE on the Texture Evolution. Figure 11 shows the (0002) and (10–10) pole figures of the studied alloy after CEE deformation by XRD in the RD-TD plane. It can be found from Figure 11 that the CEE process has an obvious influence on the texture evolution of studied AZ80 Mg alloy. Prior to the CEE process, the annealed Mg alloy shows dispersive orientation distribution for the (0002) and (10-10) lattice planes. The (0002) pole intensity is 5.3, and the (10–10) pole intensity is only 2, as shown in Figure 11(a). During the CEE process, the obviously preferred orientation is developed from Figure 10(a)–10(b). The (0002) basal texture intensity of the studied alloy first decreases and then increases with the increase of CEE passes, as shown in Figure 12. After one-pass CEE process, most of *c*-axes of the HCP lattice are nearly parallel to the ND direction, and there appears highly preferred orientation. However, the (0002) and (10–10) pole intensities slightly reduce than the one-pass CEE. During one-pass CEE process, the large number of twinning deformation causes lattice rotation and changes the grain orientation, as seen in Figure 8(a). So the texture is weakened after one-pass CEE process.

The (0002) pole intensity further decreases when the two-pass CEE takes place, while the (10–10) pole intensity increases slightly. There appear multiple basal and prismatic peaks, as shown in Figure 11(c). This can be attributed to the mixed deformation mechanisms during the two-pass CEE process. According to the discussion in Section 3.3, a mixed structure with coarse grains and fine grains is formed by RDRX. Such consequences are the fine grains can activate the nonbasal slip and grain boundary slip [36], while a few residual twinning still participates in the CEE deformation of coarse grains. The deformation mechanism becomes mixed and complex, including the basal slip, activated nonbasal slip, twinning deformation, and two kinds of DRX behaviors (RDRX and a few TDRX). Although slip deformation cannot change the grain orientation, both twinning deformation and the RDRX behavior can rotate the lattice, reduce the preferred orientation, and weaken texture [20, 30].

Strikingly, the (0002) pole intensity reaches 19 and the (10–10) texture intensity increases to 4, as shown in Figure 11(d), which implies that an extremely strong (0002) basal texture is obtained after three-pass CEE. The reason is that, after first two passes of CEE, the twinning is gradually restrained owing to the grain refinement. On the contrary, the slip deformation and CDRX mechanism are gradually dominant with the unceasing grain refinement. The slipping and CDRX mechanism cannot effectively remove or reduce the preferred orientation of CEE deformation. Eventually, the extremely intensive basal texture is formed after three-pass CEE (Figure 11(d)).

Figure 12 shows the relationships between average grain size (0002) pole intensity and number of CEE pass. It can be seen from Figure 12 that the grain size decreases successively with the increase of CEE pass, and the grain refinement effect of the first pass CEE is most striking. The (0002) pole intensity first decreases and then increases because the texture intensity is strongly related to the deformation ways and the

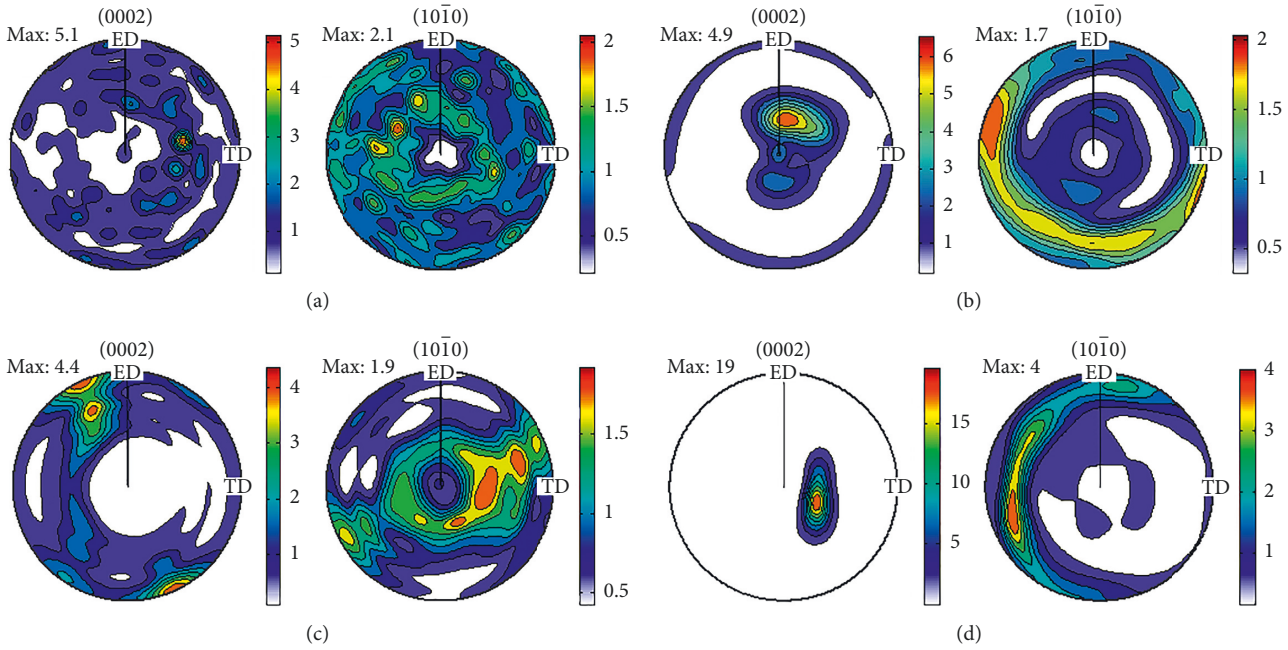

Figure 11: (0002) and (10–10) pole figures of the studied Mg alloy after CEE process: (a) as-annealed; (b) one-pass; (c) two-pass; (d) three-pass.

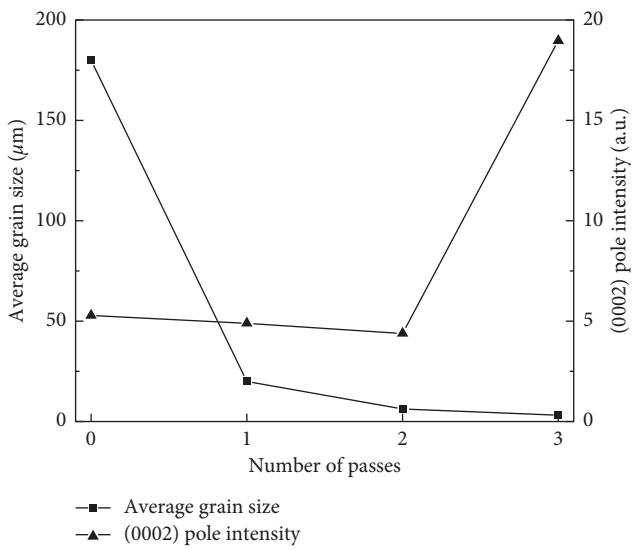

Figure 12: Relationships between average grain size, (0002) pole intensity, and number of CEE pass.

deformation mechanisms. From the above discussion, during the CEE deformation, the deformation mechanism and DRX behavior of CEE process mainly depend on grain size in this work. Twinning easily occurs within the coarse grains, while slipping is the major deformation mechanism of the fine grains. Twinning and slipping cooperate and compete with each other and coordinate the CEE deformation. It is important that twinning (or TDRX) and RDRX behavior can substantially weaken the texture intensity of the CEE alloy, but slipping and CDRX behavior cannot. With the dramatic decrease of grain size, slipping and CDRX behavior are gradually dominant, and the weakening effect of twinning and RDRX behavior on the CEE deformation texture reduces continuously. Eventually, the extremely strong (0002) basal texture is formed after three-pass CEE.

4. Conclusion

The influence of CEE process on microstructures, deformation mechanism, dynamic recrystallization behavior, and texture evolution of AZ80 magnesium alloy were investigated. Main findings are summarized as follows:

(1) The CEE process has a great effect on microstructures of the studied Mg alloy. With the increase of CEE pass, the grain size decreases continuously. The grain refinement of the one-pass CEE is the most remarkable, and there appear a large number of twins. After three-pass CEE, a well-distributed microstructure with fine equiaxed grains is obtained.

(2) With the increase of CEE pass, the deformation mechanism changes chiefly from twinning to slipping and the DRX mechanism changes mainly from TDRX to RDRX and then to CDRX, which leads to the continuous refinement of grains.

(3) The crystallographic misorientation between the new grains and matrix grains decreases gradually and a relatively small angle misorientation is obtained after three-pass CEE. The grain misorientations of the first two passes are attributed to the TDRX and RDRX behaviors, respectively. The (0002) basal texture intensity first decreases and then significantly increases, which is caused by the changes of the deformation and DRX mechanisms. After three passes of CEE deformation, the extremely strong (0002) basal texture is formed ultimately.

Data Availability

The (chemical composition of the cast AZ80 Mg alloy) data used to support the findings of this study are included within the article.

Conflicts of Interest

We declare that we have no financial and personal relationships with other people or organizations that can inappropriately influence our work, there is no professional or other personal interest of any nature or kind in any product, service, and/or company that could be construed as influencing the position presented in, or the review of, this article.

Acknowledgments

This work was supported by the Special Program for Key Basic Research of the Ministry of Science and Technology, China (Grant no. 202012CB626808) and the Natural Science Foundation of Shanxi Province, China (Grant nos. 2013011022-5, 2012011022-2). This experiment was completed in School of Materials Science and Engineering, North University of China.

References

[1] Z. Zhao, Q. Chen, C. Hu, and D. Shu, "Microstructure and mechanical properties of SPD-processed an as-cast AZ91D+Y magnesium alloy by equal channel angular extrusion and multi-axial forging," *Materials & Design*, vol. 30, no. 10, pp. 4557–4561, 2009.

[2] Y. C. Lin, Z.-H. Liu, X.-M. Chen, and J. Chen, "Uniaxial ratcheting and fatigue failure behaviors of hot-rolled AZ31B magnesium alloy under asymmetrical cyclic stress-controlled loadings," *Materials Science and Engineering: A*, vol. 573, no. 3, pp. 234–244, 2013.

[3] N. B. Tork, N. Pardis, and R. Ebrahimi, "Investigation on the feasibility of room temperature plastic deformation of pure magnesium by simple shear extrusion process," *Materials Science and Engineering: A*, vol. 560, no. 2, pp. 34–39, 2013.

[4] S. A. Askariani and S. M. Hasan Pishbin, "Hot deformation behavior of Mg-4Li-1Al alloy via hot compression tests," *Journal of Alloys and Compounds*, vol. 688, pp. 1058–1065, 2016.

[5] J. Deng, Y. C. Lin, S.-S. Li, J. Chen, and Y. Ding, "Hot tensile deformation and fracture behaviors of AZ31 magnesium alloy," *Materials & Design*, vol. 49, pp. 209–219, 2013.

[6] A. Zhilyaev and T. Langdon, "Using high-pressure torsion for metal processing: fundamentals and applications," *Progress in Materials Science*, vol. 53, no. 6, pp. 893–979, 2008.

[7] R. Z. Valiev and T. G. Langdon, "Principles of equal-channel angular pressing as a processing tool for grain refinement," *Progress in Materials Science*, vol. 51, no. 7, pp. 881–981, 2006.

[8] Q. Wang, Y. Chen, M. Liu, J. Lin, and H. J. Roven, "Microstructure evolution of AZ series magnesium alloys during cyclic extrusion compression," *Materials Science and Engineering: A*, vol. 527, no. 9, pp. 2265–2273, 2010.

[9] N. Pardis, B. Talebanpour, R. Ebrahimi, and S. Zomorodian, "Cyclic expansion-extrusion (CEE): a modified counterpart of cyclic extrusion-compression (CEC)," *Materials Science and Engineering: A*, vol. 528, no. 25-26, pp. 7537–7540, 2011.

[10] N. Pardis, C. Chen, M. Shahbaz, R. Ebrahimi, and L. S. Toth, "Development of new routes of severe plastic deformation through cyclic expansion-extrusion process," *Materials Science and Engineering: A*, vol. 613, no. 11, pp. 357–364, 2014.

[11] N. Pardis, C. Chen, R. Ebrahimi et al., "Microstructure, texture and mechanical properties of cyclic expansion-extrusion deformed pure copper," *Materials Science and Engineering: A*, vol. 628, pp. 423–432, 2015.

[12] Y. Chino, K. Kimura, and M. Mabuchi, "Twinning behavior and deformation mechanisms of extruded AZ31 Mg alloy," *Materials Science and Engineering: A*, vol. 486, no. 1-2, pp. 481–488, 2008.

[13] D. Liu, Z.-Y. Liu, and E.-D. Wang, "Evolution of twins and texture and its effects on mechanical properties of AZ31 magnesium alloy sheets under different rolling process parameters," *Transactions of Nonferrous Metals Society of China*, vol. 25, no. 11, pp. 3585–3594, 2015.

[14] G.-S. Hu, D.-F. Zhang, Y.-F. Dong, X. Chen, L.-Y. Jiang, and F.-S. Pan, "Microstructures and mechanical properties of as-extruded and heat treated Mg-6Zn-1Mn-4Sn-1.5Nd alloy," *Transactions of Nonferrous Metals Society of China*, vol. 25, no. 5, pp. 1439–1445, 2015.

[15] T. Wang, L. Jiang, R. K. Mishra, and J. J. Jonas, "Effect of Ca addition on the intensity of the rare earth texture component in extruded magnesium alloys," *Metallurgical and Materials Transactions A*, vol. 45, no. 10, pp. 4698–4709, 2014.

[16] I. J. Beyerlein, N. A. Mara, D. Bhattacharyya, D. J. Alexander, and C. T. Necker, "Texture evolution via combined slip and deformation twinning in rolled silver-copper cast eutectic nanocomposite," *International Journal of Plasticity*, vol. 27, no. 1, pp. 121–146, 2011.

[17] T. Leffer and R. R. Lay, "The brass-type texture and its deviation from the copper-type texture," *Progress in Materials Science*, vol. 54, no. 3, pp. 351–395, 2009.

[18] Y. N. Wang and J. C. Huang, "The role of twinning and untwinning in yielding behavior in hot-extruded Mg-Al-Zn alloy," *Acta Materialia*, vol. 55, no. 3, pp. 897–905, 2007.

[19] R. Xin, C. Guo, Z. Xu, G. Liu, X. Huang, and Q. Liu, "Characteristics of long {10-12} twin bands in sheet rolling of a magnesium alloy," *Scripta Materialia*, vol. 74, pp. 96–99, 2014.

[20] J. A. Valle, M. Prado, and O. A. Ruano, "Texture evolution during large-strain hot rolling of the Mg AZ61 alloy," *Materials Science and Engineering A*, vol. 355, no. 1-2, pp. 68–78, 2003.

[21] J. Peng, Z. Zhang, Y. Li, W. Zhou, and Y. Wu, "Twinning-induced dynamic recrystallization and micro-plastic mechanism during hot-rolling process of a magnesium alloy," *Materials Science and Engineering: A*, vol. 699, pp. 99–105, 2017.

[22] S. M. Fatemi-Varzaneh, A. Zarei-Hanzaki, and H. Beladi, "Dynamic recrystallization in AZ31 magnesium alloy," *Materials Science and Engineering A*, vol. 456, no. 1, pp. 52–57, 2017.

[23] H. Sheikh and R. Ebrahimi, "Investigation on texture evolution during cyclic expansion-extrusion (CEE) technique using crystal plasticity finite element modeling," *Journal of Materials Science*, vol. 51, no. 22, pp. 10178–10190, 2016.

[24] J. Koike, "Enhanced deformation mechanisms by anisotropic plasticity in polycrystalline Mg alloys at room temperature," *Metallurgical and Materials Transactions A*, vol. 36, no. 7, pp. 1689–1696, 2005.

[25] A. Jain, O. Duygulu, D. W. Brown, C. N. Tomé, and S. R. Agnew, "Grain size effects on the tensile properties and deformation mechanisms of a magnesium alloy, AZ31B, sheet," *Materials Science and Engineering: A*, vol. 486, no. 1-2, pp. 545–555, 2008.

[26] S. E. Ion, F. J. Humphreys, and S. H. White, "Dynamic recrystallisation and the development of microstructure during the high temperature deformation of magnesium," *Acta Metallurgica*, vol. 30, no. 10, pp. 1909–1919, 1982.

[27] Y. Chino, K. Kimura, M. Hakamada, and M. Mabuchi, "Mechanical anisotropy due to twinning in an extruded AZ31 Mg alloy," *Materials Science and Engineering: A*, vol. 485, no. 1-2, pp. 311–317, 2008.

[28] Z. Keshavarz and M. R. Barnett, "EBSD analysis of deformation modes in Mg-3Al-1Zn," *Scripta Materialia*, vol. 55, no. 10, pp. 915–918, 2006.

[29] A. Galiyev, R. Kaibyshev, and G. Gottstein, "Correlation of plastic deformation and dynamic recrystallization in magnesium alloy ZK60," *Acta Materialia*, vol. 49, no. 7, pp. 1199–1207, 2001.

[30] Y. Chino, K. Kimura, and M. Mabuchi, "Deformation characteristics at room temperature under biaxial tensile stress in textured AZ31 Mg alloy sheets," *Acta Materialia*, vol. 57, no. 5, pp. 1476–1485, 2009.

[31] R. Kaibyshev, A. Galiev, and O. Sitdikov, "On the possibility of producing a nanocrystalline structure in magnesium and magnesium alloys," *Nanostructured Materials*, vol. 6, no. 5–8, pp. 621–624, 1995.

[32] A. Galiyev, R. Kaibyshev, and T. Sakai, "Continuous dynamic recrystallization in magnesium alloy," *Materials Science Forum*, vol. 419–422, pp. 509–514, 2003.

[33] D. Sarker, J. Friedman, and D. L. Chen, "Twin growth and texture evolution in an extruded am30magnesium alloy during compression," *Journal of Materials Science and Technology*, vol. 30, no. 9, pp. 884–887, 2014.

[34] Y. Yoshida, L. Cisar, S. Kamado, and Y. Kojima, "Effect of microstructural factors on tensile properties of an ECAE-processed AZ31 magnesium alloy," *Materials Transactions*, vol. 44, no. 4, pp. 468–475, 2003.

[35] C. Schmidt, R. Kawalla, T. Walde, H. Riedel, A. Prakash, and C. Poizat, "Experimental and numerical investigation of texture development during hot rolling of magnesium alloy AZ31," *Materials Science Forum*, vol. 539-543, no. 2, pp. 3448–3453, 2007.

[36] R. B. Figureueiredo, F. S. J. Poggiali, C. L. P. Silva, P. R. Cetlin, and T. G. Langdon, "The influence of grain size and strain rate on the mechanical behavior of pure magnesium," *Journal of Materials Science*, vol. 51, no. 6, pp. 3013–3024, 2016.